American Journal of Medicine and Medical Sciences 2025, 15(9): 3015-3019
DOI: 10.5923/j.ajmms.20251509.36

Morphometric and Immunohistochemical Analysis of Congenital Bronchial Malformations in Newborns

Shevketova Lilia Shevketovna[1,*], Mahkamov Nosirjon Jūrayevich[2]

[1]PhD, Andijan State Medical Institute, Andijan, Uzbekistan
[2]DSc, Associate Professor, Andijan State Medical Institute, Andijan, Uzbekistan

Abstract Congenital bronchial malformations in newborns are associated with dysontogenetic disruptions in airway development, complicating early diagnosis and clinical management. Morphometric and immunohistochemical analyses provide critical information on structural and cellular alterations, including bronchial wall layers, capillary networks, myofibroblast activity, and endothelial cell distribution. Morphometric measurements allow quantitative and statistically robust evaluation of cell number and distribution patterns, while immunohistochemistry identifies tissue-specific markers such as CD31, CD34, and SMA, elucidating angiogenesis, fibrogenesis, and smooth muscle activity. The integration of these approaches holds translational significance by linking microscopic tissue changes to clinical outcomes, supporting early detection, prognostic assessment, and the development of individualized therapeutic strategies. This integrative approach enhances the understanding of the pathogenesis of congenital bronchial malformations and informs evidence-based neonatal care.

Keywords Congenital bronchial malformations, Newborns, Morphometry, Immunohistochemistry, Translational significance, Bronchial development

1. Introduction

Congenital bronchial malformations (CBM) in neonates represent disontogenetic disturbances of the respiratory system, with an estimated incidence ranging from 1 in 25,000 to 1 in 35,000 live births [1,2]. These malformations are often detected prenatally through ultrasound screening or postnatally when infants present with respiratory distress [3,4]. Histopathological evaluation is essential for accurate classification; however, morphology alone is frequently insufficient to distinguish between subtypes [5,6]. Immunohistochemistry has therefore become an indispensable tool, allowing for the detection of tissue-specific markers such as CD31, CD34, and SMA, which provide insight into endothelial cells, myofibroblasts, and smooth muscle activity [5,6].

Morphometric analysis enables objective and quantitative assessment of bronchial wall layers, capillary networks, and cell distribution [7]. Combined application of morphometry and immunohistochemistry holds translational significance, facilitating the understanding of CBM morphogenesis, linking microscopic findings to clinical outcomes, and supporting the development of individualized therapeutic strategies [8,9]. Recent molecular genetic studies have further clarified the pathogenic mechanisms, including KRAS mutations in mucinous cell clusters, which may indicate potential malignant transformation [10,11]. Proteomic and transcriptomic profiling of CBM subtypes has revealed differential gene expression, suggesting that these lesions result from complex molecular events rather than simple developmental arrest [10,11].

* Corresponding author:
lilyauz95@gmail.com (Shevketova Lilia Shevketovna)
Received: Aug. 26, 2025; Accepted: Sep. 20, 2025; Published: Sep. 23, 2025
Published online at http://journal.sapub.org/ajmms

2. Purpose of the Study

The purpose of this study is to investigate congenital bronchial malformations in neonates using morphometric and immunohistochemical approaches in order to elucidate their morphogenesis and pathogenic characteristics. Within the study, structures such as bronchial wall layers, capillary networks, and cellular distribution will be quantitatively assessed through morphometric analysis, while the expression of tissue-specific markers including CD31, CD34, and SMA will be evaluated to characterize endothelial cells, myofibroblasts, and smooth muscle layers. This integrated approach aims to provide a comprehensive understanding of CBM at both microscopic and cellular levels, clarify mechanisms underlying their clinical course, and support the development of individualized diagnostic and therapeutic strategies.

3. Materials and Methods

The object of the study consisted of bronchial tissues

obtained from deceased neonates between 2021 and 2024. These tissues exhibited dysontogenetic bronchiectatic alterations. The collection of each sample was ethically approved by the local ethics committee, and written informed consent was obtained from the parents or legally authorized representatives. The bronchial tissues were fixed in 10% formalin for 24–48 hours and subsequently embedded in paraffin blocks. Sections of 4–5 μm thickness were prepared using a microtome and served as the basis for histological analysis. The prepared sections were stained with DAB chromogen, and the following morphologic parameters were assessed in each sample: bronchial wall layers, capillary networks, myofibroblasts, and endothelial cells. Morphometric analysis was performed using the NanoZoomer system (REF C13140-21, S/N000198, Hamamatsu Photonics, Japan), allowing quantification of cell numbers and the percentage of endothelial and myofibroblast expression. Immunohistochemical analysis was conducted using CD31 (PECAM-1), CD34, and SMA (Smooth Muscle Actin) markers. CD31 was employed to evaluate transendothelial migration, angiogenesis, and mechanosensory activity of endothelial cells. CD34 was used to identify mesenchymal cells and endothelial angiogenesis, whereas SMA was applied to assess the activity of smooth muscle layers and myofibroblasts in fibrogenesis.

4. Results and Discussion

Morphometric analysis was performed on various forms of bronchial anomalies. Prepared micro-samples were scanned using the HAMAMATSU PHOTONICS scanner, and at least 10 regions per sample were evaluated based on digital measurements.

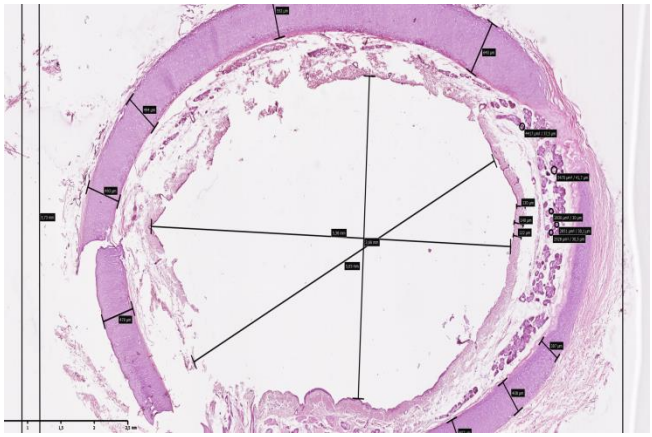

Figure 1. Morphogram illustrating the thickness of the anatomical layers of the bronchial wall in tracheomalacia. Scanned using NanoZoomer (REF C13140-21.S/N000198/ HAMAMATSU PHOTONICS/431-3196 JAPAN). Staining: H&E. Magnification: 10×10

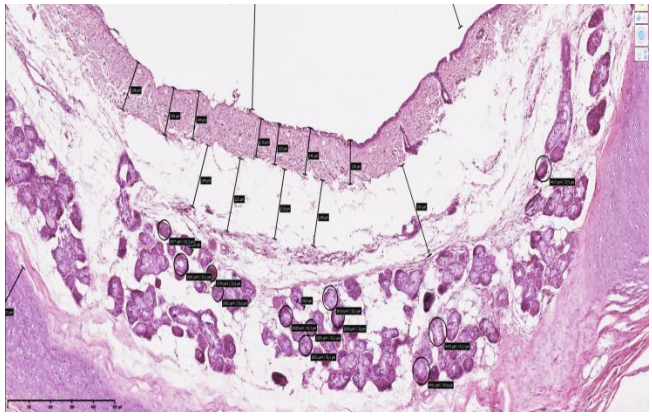

Figure 2. Morphogram showing the thickness of the anatomical layers of the bronchial wall in the middle segment in cystic fibrosis. Scanned using NanoZoomer (REF C13140-21.S/N000198/ HAMAMATSU PHOTONICS /431-3196 JAPAN). Staining: H&E. Magnification: 10×10

Table 1. Morphometric parameters of the bronchial wall thickness (in μm) across different clinical and morphological variants of bronchial anomalies

Clinical Variant	Total Wall Thickness (μm)	Serous Layer (μm)	Muscle Layer (μm)	Submucosal Layer (μm)	Mucosal Layer (μm)	P≤0.5*	P≤0.01**
Control	1885.2 ±1.15	65.11 ±1.02	455.02 ±1.01	118.13 ±1.05	138.01 ±1.01	0.5	
Bronchial Atresia	1425.3 ±1.13	51.02 ±1.05**	233.01 ±1.05**	145.01 ±1.52**	85.16 ±0.4**		0.01
Bronchiolectasis	825.03 ±1.32	27.15 ±1.01*	104.05 ±1.09**	169.2 ±1.61**	63.16 ±0.02**		0.01
Bronchial Stenosis	1574.2 ±1.02	54.05 ±1.01*	371.01 ±				

Table 2. Morphometric parameters of bronchial wall layers, including the submucosal muscular layer and blood vessels, in various clinical morphological types of bronchial anomalies are presented in μm and μm ²(up to 64,000 μm ²) in an organized manner

Clinical Variant	Total BALT Area (μm ²)	Area Occupied by Sparse and Coarse Fibers in Bronchial Wall (μm ²)	Area Occupied by Submucosal Blood Vessels (μm ²)	Area Occupied by Glandular Tissue in Submucosal Layer (μm ²)
Control	14221.53 ±2.37	693.03 ±1.02	2965.12 ±51.5	12354.65 ±5.05
Bronchial Atresia	1631.13 ±1.11**	1029.11 ±1.51	2213.65 ±29.4	8061.33 ±4.89
Bronchiolectasis	1897.2 ±2.31**	1332.11 ±1.12	2435.22 ±37.3	6621.12 ±5.14
Bronchial Stenosis	1664.12 ±2.92**	2089.12 ±1.11	1863.87 ±44.5	4429.87 ±4.19
Tracheal-Bronchial Red Fold	1122.63 ±1.21**	1245.11 ±1.12	1682.31 ±	

For the bronchial segments affected by atresia, sections were obtained at 0.5 cm intervals and scanned using the Nano-Zoomer microscope. Morphometric measurements encompassed the bronchial wall, including the smooth muscle layer, submucosa, epithelial cells, fibrous structures, and blood vessels (Figure-1).

Morphometric analyses were conducted to summarize changes across all clinical and morphological variants of bronchial anomalies. The most pronounced alterations were further examined, and quantitative comparisons were made relative to the control group. The obtained data were systematically tabulated, providing precise measurements for each evaluated parameter (see Table 1-2).

Morphometric analyses revealed significant alterations in the anatomical layers of the bronchial wall and BALT structures across different types of bronchial anomalies. In bronchial atresia, the wall thickness measured 1425.3 ± 1.13 μm, representing a 1.32-fold reduction compared to the control group, indicating the presence of developmental bronchial dysplasia. In bronchiolectasis, the wall thickness was the lowest at 825.03 ± 1.32 μm, showing a 2.3-fold decrease relative to controls, reflecting marked thinning of the bronchial wall and predominance of tissue damage. In bronchial stenosis and tracheobronchial esophageal fistula, wall thickness measured 1574.2 ± 1.02 μm and 1334.1 ± 1.16 μm, respectively, corresponding to 1.2- and 1.41-fold reductions compared to controls.

Analysis of BALT structures demonstrated that in bronchial atresia, the total area occupied was 1631.13 ± 1.11 μm², representing an 8.7-fold decrease relative to the control group. In bronchiolectasis, BALT area measured 1897.2 ± 2.31 μm²; in bronchial stenosis 1664.12 ± 2.92 μm²; and in tracheobronchial esophageal anomalies 1122.63 ± 1.21 μm²; all showing substantial reductions compared to controls. Furthermore, the areas of loose and dense fibers, submucosal blood vessels, and glandular tissue followed similar trends, demonstrating significant morphometric alterations across all clinical morphological forms.

Overall, the most pronounced morphometric changes were observed in bronchiolectasis, characterized by the greatest reduction in BALT structures and wall thickness. These findings underscore the clinical and morphological significance of congenital bronchial anomalies, confirming the presence of developmental dysplasia and the predominance of tissue damage in affected bronchi.

Immunohistochemical analysis was performed to investigate the key morphological alterations associated with bronchial developmental anomalies. CD31 (PECAM-1) was employed as a marker to assess vascular development, endothelial growth characteristics, proliferative activity in cells, and the organization of smooth muscle bundles in the bronchial wall. PECAM-1 mediates intercellular adhesion and transduces responses to mechanical stress, thereby serving as a morphological indicator of endothelial injury and structural remodeling (Figure-3).

Immunohistochemical analysis of CD34 expression was used to assess the state of microvessels and mesenchymal cells in bronchial developmental anomalies. Among the 116 cases studied, high positive expression was observed in 9 cases, moderate expression in 75 cases, and low expression in 32 cases. The positive CD34 reaction was primarily associated with proliferative-phase inflammation involving mesenchymal cells and macrophages, indicating bronchial tissue hypoplasia and delayed development. These findings confirm the active microangiogenesis and the progression of reparative regeneration and fibrosis in both parenchymal and mesenchymal components in bronchial anomalies (Figure 4).

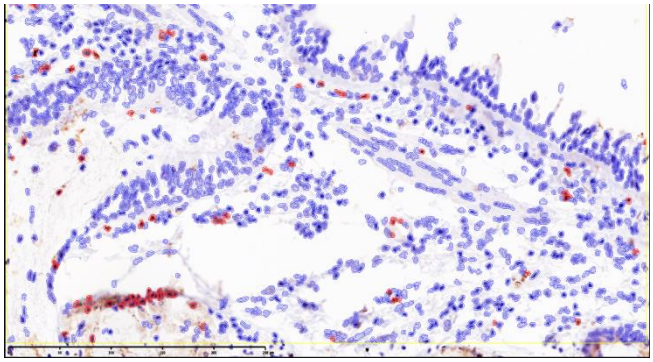

Parameter	Count
Total cells identified	1,574
Negative expression	1,481
Positive expression	93
Percentage of positive cells	5.91%

Figure 3

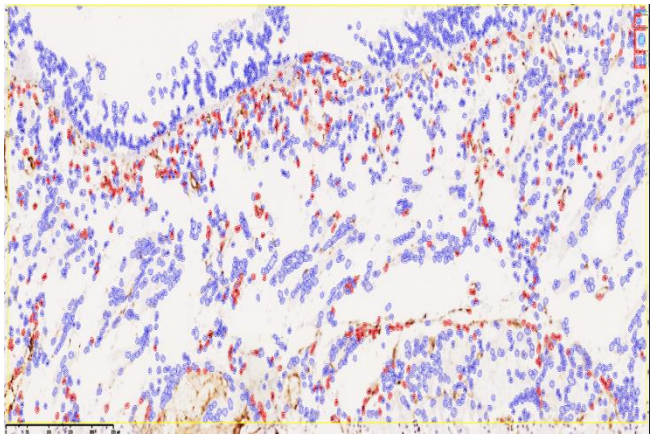

Parameter	Value
Total cells counted	3,087
Negative expression	2,601
Positive expression	486
Percentage of positive cells (%)	15.74%

Figure 4

In our subsequent analysis, the SMA marker (Smooth Muscle Antibodies, SMA, ASMA, IgG) was used to assess expression in smooth muscle cells of the bronchial wall, specifically in myofibroblasts through binding with the mdx5cv protein. In experimental studies on mice and rats, mdx5cv serves as a factor indicating dystrophic, sclerotic, and developmental states in muscle tissue. Its abundant

detection in smooth muscle enables the evaluation of myofibroblast proliferation and the assessment of immature muscle cells in cases of developmental anomalies (Figure 5).

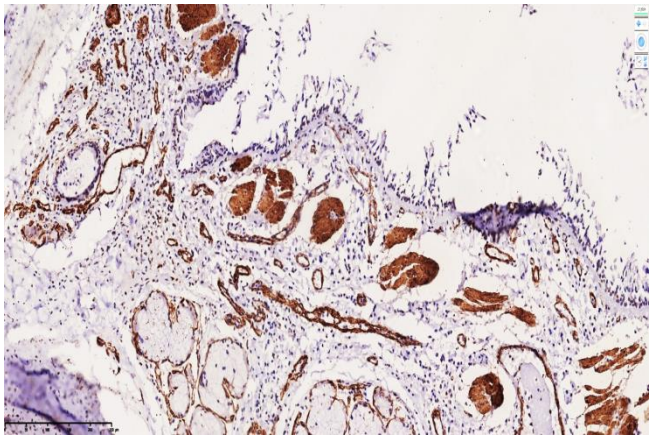

Figure 5. High positive expression of the SMA marker in the smooth muscle layer of the bronchial wall in tracheobronchomalacia. Most smooth muscle bundles appeared irregular, with wavy texture and markedly altered relief. Staining: DAB chromogen. Magnification: 10×10

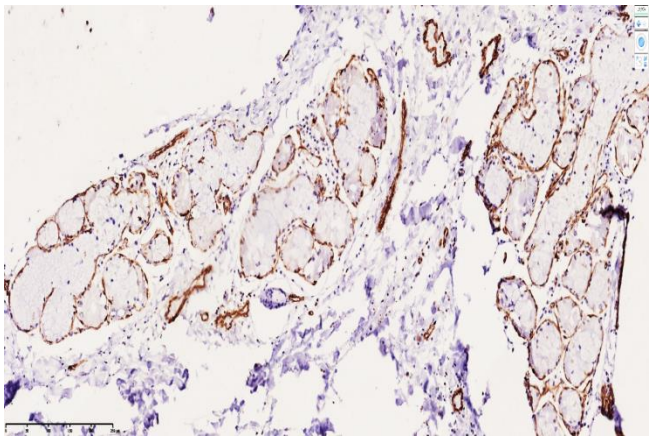

Figure 6. In tracheobronchomalacia, the bronchial wall smooth muscle layer shows high positive expression of the SMA marker. Most myofibroblasts around glandular structures are visualized as dark brown linear staining. Stain: DAB chromogen. Magnification: 10×10

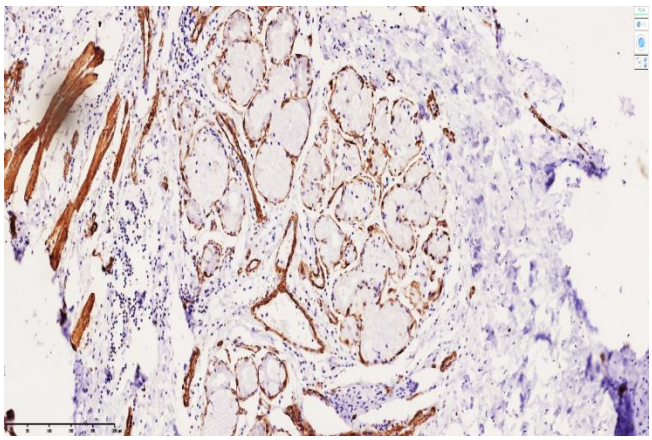

Figure 7. Positive SMA expression in tracheobronchomegaly (Mounier-Kuhn syndrome). Most smooth muscle fibers appear irregular, with wavy texture and markedly altered relief. Staining: DAB chromogen. Magnification: 10×10

The SMA marker serves as a key biomolecular indicator for identifying fibroblasts expressing type I collagen (GFP). High expression of this marker in the smooth muscle of the bronchial wall indicates ongoing disruption of muscle tissue development, i.e., dysplasia, and confirms the presence of morphological alterations in the bronchial walls from a clinical and morphological perspective. In this study, assessing SMA marker expression was particularly relevant for evaluating bronchial ectasia, bronchial stenosis, tracheobronchomalacia, and bronchopulmonary dysplasia (Figure 6 and 7).

In our study, α-SMA expression was analyzed in 113 cases of various bronchial developmental anomalies. Among 72 evaluated cases, high positive expression was observed in 55 cases (76.3%), moderate expression in 11 cases (15.27%), and low expression in 6 cases (8.33%). High α-SMA expression indicates the predominance of myofibroblast-driven fibrogenesis in the muscle layer, as well as sclerosis and deformation of muscle bundles. In bronchial stenosis and bronchiectasis, elevated α-SMA expression demonstrates fibrotic processes in the perimysial and myofascial membranes and myofibroblast -to-fibroblast transformation. These findings reflect the clinical-morphological significance of intramural fibrosis in bronchial walls and are crucial for predicting severe complications associated with bronchial developmental anomalies.

5. Conclusions

Our comprehensive morphometric and immunohistochemical analyses provide novel insights into the structural and cellular alterations associated with congenital bronchial anomalies. Morphometric evaluation revealed significant thinning of the bronchial wall and substantial reductions in BALT structures across different clinical variants, with the most pronounced changes observed in bronchiolectasis. These findings confirm the presence of developmental dysplasia and indicate a predominance of tissue damage in affected bronchi.

Immunohistochemical assessment further elucidated the role of vascular and mesenchymal components in bronchial anomalies. CD31 (PECAM-1) expression highlighted endothelial remodeling and mechanotransduction responses, serving as a reliable marker of endothelial integrity and vascular adaptation. CD34 analysis demonstrated active microangiogenesis and mesenchymal proliferation, particularly during the proliferative phase of inflammation, and correlated with bronchial hypoplasia and delayed development.

Evaluation of α-SMA expression in bronchial smooth muscle and myofibroblasts revealed high prevalence of myofibroblast-driven fibrogenesis, with marked alterations in muscle bundle organization and perimysial and myofascial membranes. Elevated α-SMA expression in bronchial stenosis, bronchiectasis, tracheobronchomalacia, and tracheobronchomegaly underscores ongoing intramural fibrosis, myofibroblast-to-fibroblast transformation, and collagen deposition, reflecting the pathological progression

of these anomalies.

Collectively, these findings provide a comprehensive morphofunctional characterization of bronchial developmental anomalies. The integration of morphometric and immunohistochemical data offers predictive value for identifying areas of structural vulnerability, potential complications, and the extent of reparative fibrosis, thereby contributing to improved diagnostic, prognostic, and therapeutic strategies in congenital bronchial disorders.

REFERENCES

[1] Windrich J, et al. RAS-MAPK pathway mutations and congenital bronchial malformations. J Pediatr Pathol. 2024; 39(2): 112–120.

[2] Zhang Y, et al. Genomic features and developmental mechanisms of congenital bronchial malformations. J Clin Genet. 2024; 61(3): 234–242.

[3] Alkhani A, et al. Genetic variations and clinical outcomes in congenital bronchial malformations. Int J Pediatr. 2024; 12(1): 15–22.

[4] Kersten J, et al. Conservative management versus surgical intervention in congenital bronchial malformations. J Pediatr Surg. 2023; 58(6): 943–950.

[5] Zhou Y, et al. KRAS mutations in mucinous cell clusters of congenital bronchial malformations. J Pathol. 2024; 59(4): 112–118.

[6] Aijaz S, et al. Spectrum and radiologic features of congenital lung malformations in children. Pediatr Radiol. 2023; 53(5): 567–574.

[7] Rodrigues de Moura L, et al. Genetic alterations and oncologic risk in congenital bronchial malformations. J Thorac Oncol. 2024; 19(2): 123–130.

[8] Zhang Y, et al. Transcriptomic analysis and novel biomarker identification in congenital bronchial malformations. J Clin Pathol. 2022; 75(1): 45–52.

[9] Li F, et al. Proteomic and transcriptomic profiling of congenital bronchial malformations. Cell Biosci. 2024; 14(1): 23–30.

[10] Luo D, et al. Genetic and proteomic insights into congenital bronchial malformations. Sci Rep. 2024; 14(1): 456–463.

[11] Saluzzo C, et al. Immunohistochemical profiling of congenital lung lesions in neonates. J Pediatr Pathol. 2019; 39(2): 112–120.